Earth, Planets and Space

The 2018 Hokkaido Eastern Iburi Earthquake and Hidaka arc-arc collision system

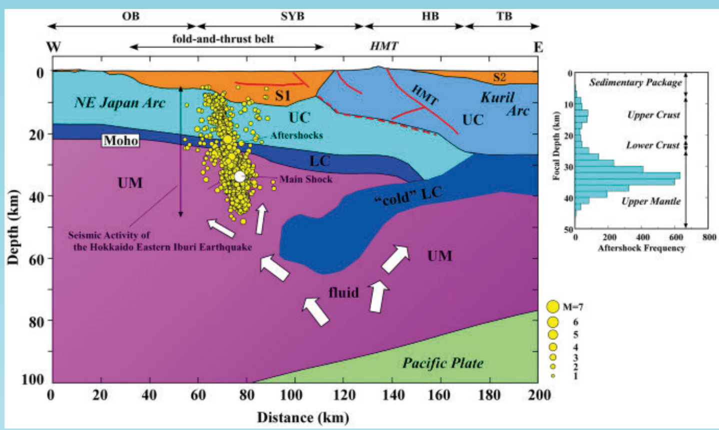

Society of Geomagnetism and Earth, Planetary and Space Sciences (SGEPSS)
The Seismological Society of Japan
The Volcanological Society of Japan
The Geodetic Society of Japan
The Japanese Society for Planetary Sciences

Japan Geoscience Union

SpringerOpen

Journal Scope

Earth, Planets and Space (EPS) is the official journal of Society of Geomagnetism and Earth, Planetary and Space Sciences, The Seismological Society of Japan, The Volcanological Society of Japan, The Geodetic Society of Japan, and The Japanese Society for Planetary Sciences.
EPS is a peer-reviewed, open-access journal published under SpringerOpen. It is an international journal covering scientific articles in the entire field of earth and planetary sciences, particularly geomagnetism, aeronomy, space science, seismology, volcanology, geodesy, and planetary science. EPS also welcomes articles in new and interdisciplinary subjects, and technical reports on instrumentation and software.

The journal was launched in 1998 and has since published over 3500 articles. All of them are available for free on SpringerLink:
https://link.springer.com/journal/40623/volumes-and-issues

More information about the journal, its article collections, and the submission process is available on the journal homepage:
https://earth-planets-space.springeropen.com

Submit your next research article to Earth, Planets and Space via:
https://www.editorialmanager.com/epsp

Yours sincerely,

Prof. Takeshi Sagiya
Editor-in-Chief, *Earth, Planets and Space*
eic@earth-planets-space.org

Earth, Planets and Space

Takahashi *et al. Earth, Planets and Space (2020) 72:65*
https://doi.org/10.1186/s40623-020-01176-4

PREFACE

Open Access

Special issue "The 2018 Hokkaido Eastern Iburi Earthquake and Hidaka arc–arc collision system"

Hiroaki Takahashi[1*], Nobuo Takai[2], Masahiro Chigira[3], Guojie Meng[4], Saeko Kita[5] and Takuji Yamada[6]

The 2018 Hokkaido Iburi Eastern Earthquake on 9 September 2018 was an inland moderate-sized Mw6.6 earthquake. The maximum intensity of VII, which is the highest in JMA intensity scale, was observed in the vicinity of the epicenter. This earthquake resulted in over 40 deaths, most of which were caused by enormous seismically induced landslides. Strong shaking also destroyed electric power facilities, causing a long-term electrical power outage throughout the Hokkaido region. This special issue focuses on describing this unique earthquake and discussing the characteristics of the seismic source process, strong ground motions, aftershock activity, tectonic background, and other related phenomena.

The source process and fault model of the earthquake have been reported in the following papers. Kobayashi et al. (2019a) suggested the steeply dipping rectangular fault at depths of 15–30 km using GNSS and InSAR geodetic data. Kobayashi et al. (2019b), Asano and Iwata (2019), and Kubo et al. (2020) discussed the rupture process in detail using strong motion data and suggested the existence of major slip at depths of 20–30 km, approximately 10 km shallower than the hypocenter. Additionally, Asano and Iwata (2019) simulated the seismic wavefield using a 3-D velocity model to reflect the complex subsurface structure of the focal region.

Katsumata et al. (2019) indicated that the rupture initiated in the deepest part of the aftershock region using local seismic network data with a 3-D velocity structure. They also suggested that the aftershock area consisted of three segments, which reflects a complex rupture process. The aftershock distribution and the estimated fault model were not consistent with the configuration of a nearby major active fault (the Ishikari–Teichi–Toen fault). Ohtani and Imanishi (2019) and Kobayashi (2019a, b) assessed the possible build-up of stress on this adjoining major active fault owing to co- and post-seismic crustal deformation, and the statistical characteristics of the seismic activity before and after the mainshock were investigated by Kumazawa et al. (2019) using the ETAS model.

The strong ground motions due to this event were accurately recorded by the dense nationwide seismographic network. Dhakal et al. (2019) found large PGAs and PGVs at a medium distance relative to the standard distance attenuation model. Nakano and Kawase (2019) suggested that the observed stress drop corresponded to the upper limit of a crustal earthquake. Dhakal et al. (2019) and Nakano and Kawase (2019) also reported nonlinear site amplification at seismic stations near the epicenter. Takai et al. (2019) concluded that the destructive strong shaking observed in the town of Mukawa resulted from the local and shallow underground structure based on subsurface structure surveys. The seismic source properties and amplification characteristics described herein provide insights that can lead to the better evaluation of strong ground motions.

The regional subsurface structure within the Hidaka collision system was investigated using seismic and magnetotelluric data. Iwasaki et al. (2019) illustrated that the Hidaka collision zone consists of a complex

*Correspondence: hiroaki@sci.hokudai.ac.jp
[1] Institute of Seismology and Volcanology, Faculty of Science, Hokkaido University, Sapporo, Japan
Full list of author information is available at the end of the article

crustal and upper mantle structure using controlled source seismic data and suggested that the mainshock and a number of aftershocks occurred in the upper mantle. Kita (2019) indicated that the relocated aftershocks determined by a regional seismic network were situated in an anomalously thick crust and were distributed near the boundaries of velocity and Qp attenuation structures. Nakamura and Shiina (2019) also suggested that a Qs boundary corresponded to the aftershock alignment. Ichihara et al. (2019) presented the heterogeneous electrical resistivity structure of the Hidaka collision zone and suggested a possible conductive zone in the aftershock region. Ikeda and Takagi (2019) observed a coseismic velocity reduction as well as possible crack formation in the focal region. Iwasaki et al. (2019) and Kita (2019) suggested that low heat flow was the cause of the anomalously deep rupture.

Ohzono et al. (2019) revealed a relatively high strain rate in the focal region using GNSS data and suggested that the presence of weak crustal material in the fold–thrust zone leads to strain accumulation. Ito et al. (2019) illustrated the possible convergence of tectonic blocks in northern Hokkaido from regional GNSS data, where the northern continuation of the focal region is located. These geodetic data suggest the regional and constant build-up of stress in central Hokkaido.

The topographic characteristics of seismically induced landslides were assessed by Kasai and Yamada (2019), who indicated that the slip surfaces of numerous shallow landslides formed in the remains of volcanic soil deposited 9000 year BP. The landslides resulting from this earthquake were more clustered, more numerous, and larger in scale than were expected from the magnitude of the earthquake. Fujiwara et al. (2019) reported linear surface ruptures with small displacements from InSAR images; they also extracted liquefaction areas and landslides using InSAR mapping data. Shibata et al. (2020) reported coseismic groundwater-level changes in wells.

This special issue presents the characteristics of the 2018 Hokkaido earthquake. It also presents the tectonic implications as well as clues for seismic hazard assessments. This Mw6.6 earthquake demonstrated that even a moderate-sized earthquake can halt social activity in Japan, which is equipped with advanced earthquake disaster countermeasures. The possible accumulation of stress on nearby major active faults provides important information regarding disaster preparedness. Further investigations of the complex Hidaka collision zone from geoscientific and earthquake engineering perspectives are expected in future work, which will improve existing disaster countermeasures.

Abbreviations

JMA: Japan Metrological Agency; GNSS: Global Navigation Satellite System; ETAS: Epidemic type aftershock sequences; PGA: Peak ground acceleration; PGV: Peak ground velocity; Qs: S-wave attenuation; Qp: P-wave attenuation; SAR: Synthetic aperture radar; InSAR: Interferometric SAR.

Acknowledgements

We are very grateful to the authors who submitted papers to the special issue and to the referees, who provided valuable suggestions and recommendations. We are also thankful to the Editor-in-Chief, Dr. Ogawa and Dr. Furuya who recommended for the organization of this special issue.

Authors' contributions

HT, NT, MC, GM, SK and TY served as guest editors for this special issue. All authors read and approved the final manuscript.

Competing interests

The authors declare that they have no competing interests.

Author details

[1] Institute of Seismology and Volcanology, Faculty of Science, Hokkaido University, Sapporo, Japan. [2] Faculty of Engineering, Hokkaido University, Sapporo, Japan. [3] Disaster Prevention Research Institute, Kyoto University, Uji, Japan. [4] Institute of Earthquake Forecasting, China Earthquake Administration, Beijing, China. [5] Building Research Institute, Tsukuba, Japan. [6] Faculty of Science, Ibaraki University, Mito, Japan.

Received: 10 April 2020 Accepted: 14 April 2020
Published online: 13 May 2020

References

Asano K, Iwata T (2019) Source rupture process of the 2018 Hokkaido Eastern Iburi earthquake deduced from strong-motion data considering seismic wave propagation in three-dimensional velocity structure. Earth Planets Space 71:101. https://doi.org/10.1186/s40623-019-1080-0

Dhakal YP, Kunugi T, Kimura T et al (2019) Peak ground motions and characteristics of nonlinear site response during the 2018 Mw 6.6 Hokkaido eastern Iburi earthquake. Earth Planets Space 71:56. https://doi.org/10.1186/s40623-019-1038-2

Fujiwara S, Nakano T, Morishita Y et al (2019) Detection and interpretation of local surface deformation from the 2018 Hokkaido Eastern Iburi Earthquake using ALOS-2 SAR data. Earth Planets Space 71:64. https://doi.org/10.1186/s40623-019-1046-2

Ichihara H, Mogi T, Satoh H et al (2019) Electrical resistivity modeling around the Hidaka collision zone, northern Japan: regional structural background of the 2018 Hokkaido Eastern Iburi earthquake (Mw 6.6). Earth Planets Space 71:100. https://doi.org/10.1186/s40623-019-1078-7

Ikeda H, Takagi R (2019) Coseismic changes in subsurface structure associated with the 2018 Hokkaido Eastern Iburi Earthquake detected using autocorrelation analysis of ambient seismic noise. Earth Planets Space 71:72. https://doi.org/10.1186/s40623-019-1051-5

Ito C, Takahashi H, Ohzono M (2019) Estimation of convergence boundary location and velocity between tectonic plates in northern Hokkaido inferred by GNSS velocity data. Earth Planets Space 71:86. https://doi.org/10.1186/s40623-019-1065-z

Iwasaki T, Tsumura N, Ito T et al (2019) Structural heterogeneity in and around the fold-and-thrust belt of the Hidaka Collision zone, Hokkaido, Japan and its relationship to the aftershock activity of the 2018 Hokkaido Eastern Iburi Earthquake. Earth Planets Space 71:103. https://doi.org/10.1186/s40623-019-1081-z

Kasai M, Yamada T (2019) Topographic effects on frequency-size distribution of landslides triggered by the Hokkaido Eastern Iburi Earthquake in 2018. Earth Planets Space 71:89. https://doi.org/10.1186/s40623-019-1069-8

Katsumata K, Ichiyanagi M, Ohzono M et al (2019) The 2018 Hokkaido Eastern Iburi earthquake (M_{JMA} = 6.7) was triggered by a strike-slip faulting in a stepover segment: insights from the aftershock distribution and the focal mechanism solution of the main shock. Earth Planets Space 71:53. https://doi.org/10.1186/s40623-019-1032-8

Kita S (2019) Characteristics of relocated hypocenters of the 2018 M6.7 Hokkaido Eastern Iburi earthquake and its aftershocks with a three-dimensional seismic velocity structure. Earth Planets Space 71:122. https://doi.org/10.1186/s40623-019-1100-0

Kobayashi H, Koketsu K, Miyake H (2019a) Rupture process of the 2018 Hokkaido Eastern Iburi earthquake derived from strong motion and geodetic data. Earth Planets Space 71:63. https://doi.org/10.1186/s40623-019-1041-7

Kobayashi T, Hayashi K, Yarai H (2019b) Geodetically estimated location and geometry of the fault plane involved in the 2018 Hokkaido Eastern Iburi earthquake. Earth Planets Space 71:62. https://doi.org/10.1186/s40623-019-1042-6

Kubo H, Iwaki A, Suzuki W et al (2020) Estimation of the source process and forward simulation of long-period ground motion of the 2018 Hokkaido Eastern Iburi, Japan, earthquake. Earth Planets Space 72:20. https://doi.org/10.1186/s40623-020-1146-z

Kumazawa T, Ogata Y, Tsuruoka H (2019) Characteristics of seismic activity before and after the 2018 M6.7 Hokkaido Eastern Iburi earthquake. Earth Planets Space 71:130. https://doi.org/10.1186/s40623-019-1102-y

Nakamura R, Shiina T (2019) Three-dimensional S-wave attenuation structure in and around source area of the 2018 Hokkaido Eastern Iburi Earthquake, Japan. Earth Planets Space 71:114. https://doi.org/10.1186/s40623-019-1095-6

Nakano K, Kawase H (2019) Source parameters and site amplifications estimated by generalized inversion technique: focusing on the 2018 Hokkaido Iburi-Tobu earthquake. Earth Planets Space 71:66. https://doi.org/10.1186/s40623-019-1047-1

Ohtani M, Imanishi K (2019) Seismic potential around the 2018 Hokkaido Eastern Iburi earthquake assessed considering the viscoelastic relaxation. Earth Planets Space 71:57. https://doi.org/10.1186/s40623-019-1036-4

Ohzono M, Takahashi R, Ito C (2019) Spatiotemporal crustal strain distribution around the Ishikari-Teichi-Toen fault zone estimated from global navigation satellite system data. Earth Planets Space 71:50. https://doi.org/10.1186/s40623-019-1024-8

Shibata T, Takahashi R, Takahashi H et al (2020) Coseismic changes in groundwater level during the 2018 Hokkaido Eastern Iburi earthquake. Earth Planets Space 72:23. https://doi.org/10.1186/s40623-020-01152-y

Takai N, Shigefuji M, Horita J et al (2019) Cause of destructive strong ground motion within 1–2 s in Mukawa town during the 2018 Mw 66 Hokkaido eastern Iburi earthquake. Earth Planets Space 71:67. https://doi.org/10.1186/s40623-019-1044-4

Publisher's Note

FRONTIER LETTER **Open Access**

Structural heterogeneity in and around the fold-and-thrust belt of the Hidaka Collision zone, Hokkaido, Japan and its relationship to the aftershock activity of the 2018 Hokkaido Eastern Iburi Earthquake

Takaya Iwasaki*, Noriko Tsumura, Tanio Ito, Kazunori Arita, Makoto Matsubara, Hiroshi Sato, Eiji Kurashimo, Naoshi Hirata, Susumu Abe, Katsuya Noda, Akira Fujiwara, Shinsuke Kikuchi and Kazuko Suzuki

Earth, Planets and Space 2019, **71**, 103 DOI: 10.1186/s40623-019-1081-z
Received: 10 March 2019, Accepted: 11 September 2019, Published: 27 September 2019

Abstract

The Hokkaido Eastern Iburi Earthquake (M = 6.7) occurred on Sep. 6, 2018 in the southern part of Central Hokkaido, Japan. Since Paleogene, this region has experienced the dextral oblique transpression between the Eurasia and North American (Okhotsk) Plates and the subsequent collision between the Northeast Japan Arc and the Kuril Arc due to the oblique subduction of the Pacific Plate. This earthquake occurred beneath the foreland fold-and-thrust belt of the Hidaka Collision zone developed by the collision process, and is characterized by its deep focal depth (~ 37 km) and complicated rupture process. The reanalyses of controlled source seismic data collected in the 1998–2000 Hokkaido Transect Project revealed the detailed structure beneath the fold-and-thrust belt, and its relationship with the aftershock activity of this earthquake. Our reflection processing using the CRS/MDRS stacking method imaged for the first time the lower crust and uppermost mantle structures of the Northeast Japan Arc underthrust beneath a thick (~ 5–10 km) sedimentary package of the fold-and-thrust belt. Based on the analysis of the refraction/wide-angle reflection data, the total thickness of this Northeast Japan Arc crust is only 16–22 km. The Moho is at depths of 26–28 km in the source region of the Hokkaido Eastern Iburi Earthquake. Our hypocenter determination using a 3D structure model shows that most of the aftershocks are distributed in a depth range of 7–45 km with steep geometry facing to the east. The seismic activity is quite low within the thick sediments of the fold–thrust belt, from which we find no indication on the relationship of this event with the shallow (< 10–15 km) and rather flat active faults developed in the fold-and-thrust belt. On the other hand, a number of aftershocks are distributed below the Moho. This high activity may be caused by the cold crust delaminated from the Kuril Arc side by the arc–arc collision, which prevents the thermal circulation and cools the forearc uppermost mantle to generate an environment more favorable for brittle fracture.

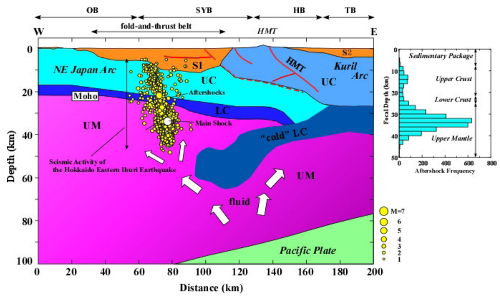

Graphical abstract

Keywords: The Hokkaido Eastern Iburi Earthquake, Hokkaido, Arc–arc collision, Fold-and-thrust belt, Seismic structure, Controlled source seismic experiments

*Corresponding author: Takaya Iwasaki, iwasaki@eri.u-tokyo.ac.jp

FULL PAPER **Open Access**

Peak ground motions and characteristics of nonlinear site response during the 2018 Mw 6.6 Hokkaido eastern Iburi earthquake

Yadab P. Dhakal*, Takashi Kunugi, Takeshi Kimura, Wataru Suzuki and Shin Aoi

Earth, Planets and Space 2019, **71**, 56 DOI: 10.1186/s40623-019-1038-2
Received: 21 January 2019, Accepted: 13 May 2019, Published: 22 May 2019

Abstract

The observed peak ground accelerations and peak ground velocities (PGVs) of the 2018 Mw 6.6 Hokkaido eastern Iburi earthquake generally followed the median values from ground motion prediction equations with reasonable errors at fault distances ≥ 50 km. However, at smaller distances, the equations significantly underestimated the peak ground motions, and it was eminent for PGVs. A comparison of surface-to-borehole spectral ratios of S-waves during the mainshock and other events revealed that the sites at smaller distances experienced various degrees of nonlinear site response. The two most widely known characteristics of nonlinear site response are the weakening of higher-frequency components and shifting of predominant frequencies to lower ones in comparison with the linear site response. At one of the sites that recorded the largest intensity of 7 in JMA scale of 0–7, the latter nonlinear effect was so dominant that the ground motions around the new predominant frequency got intensified by one order of magnitude in comparison with that during the weak-motions. Two sites, which were closely located, recorded vertical peak ground accelerations exceeding 1 g for the up-going motions. The recordings showed asymmetric waveforms and amplitudes characteristics of the nonlinear site response in extreme vertical ground motions recorded during a few earthquakes in the past. Few sites having lower vertical peak ground accelerations were also suspected of being experienced nonlinear site response on vertical motions. These findings suggest taking a cautious approach to enumerate the reduction in amplification at higher frequencies using the single-station horizontal-to-vertical (H-to-V) spectral ratio technique. However, we found that the H-to-V technique was still useful to detect nonlinearity. Finally, an ad hoc equation was derived to correct the nonlinear site amplification in predicting horizontal PGVs with respect to one of the most widely used attenuation models in Japan. The results indicated that the effect was much stronger for a larger input motion than that for a proportional change in the Vs30 values.

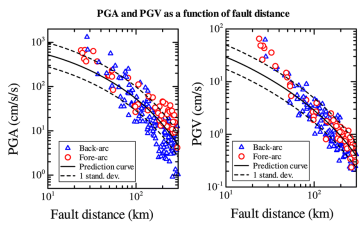

Graphical abstract

Keywords: Nonlinear site response, Degree of nonlinearity, Ground motion prediction equations, Spectral ratios, Peak ground acceleration, Peak ground velocity, The 2018 Hokkaido eastern Iburi earthquake

*Corresponding author: Yadab P. Dhakal, ydhakal@bosai.go.jp

FULL PAPER Open Access

Seismic potential around the 2018 Hokkaido Eastern Iburi earthquake assessed considering the viscoelastic relaxation

Makiko Ohtani* and Kazutoshi Imanishi

Earth, Planets and Space 2019, **71**, 57 DOI: 10.1186/s40623-019-1036-4
Received: 29 January 2019, Accepted: 13 May 2019, Published: 22 May 2019

Abstract

The 2018 M_j 6.7 Hokkaido Eastern Iburi earthquake (Iburi earthquake) occurred near the eastern boundary fault zone of the Ishikari lowlands, which is composed of a northern and southern fault. Aftershock distribution suggests the existence of a previously unknown fault (the Shallow Iburi (SI) fault) at a shallower extension of the Iburi earthquake fault. In the present study, we examined the seismic potential of the northern, southern, and SI faults based on seismological analysis and numerical simulations. The aftershock focal mechanisms infer the present-day stress field that is characterized by an ENE–SWS compression around the target faults. Slip tendency analysis shows that all target faults originally have high slip potential under the estimated stress field. We, therefore, evaluated earthquake occurrence potential on the target faults influenced by the Iburi earthquake based on the Coulomb stress (ΔCFF). We consider postseismic viscoelastic deformation in the viscoelastic medium with a three-dimensional structure. The present paper shows one possible scenario based on a model incorporating information currently available. The most of the entire SI fault was brought closer to rupture just after the earthquake, indicated by the positive ΔCFF, which is consistent with the activation of seismicity in this region. The ΔCFF continues to increase over many years after the earthquake, which may imply a growing risk of seismic hazards along the SI fault. The distribution of the ΔCFF along the southern fault and the southern half of the northern fault is characterized by a similar depth-dependent pattern. The faults were brought closer to rupture just after the earthquake, indicated by the positive ΔCFF, except for mid-depths along the faults. Then, the ΔCFF increases at shallow depths for a few decades after the earthquake, which suggests a continuous build-up of stress. Although the ΔCFF decreases at the deep depths for a few decades after the earthquake, it is insufficient to return the stress level to that before the earthquake. These results suggest that all target faults are in the state of increasing seismic risk after the Iburi earthquake.

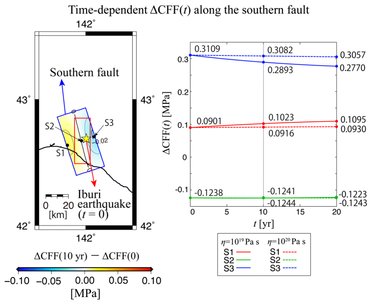

Graphical abstract

Keywords: 2018 Hokkaido Eastern Iburi earthquake, Seismic potential, Stress field estimation, Slip tendency analysis, Time-dependent Coulomb stress, Viscoelastic relaxation

*Corresponding author: Makiko Ohtani, ohtani.m@aist.go.jp

FULL PAPER Open Access

Rupture process of the 2018 Hokkaido Eastern Iburi earthquake derived from strong motion and geodetic data

Hiroaki Kobayashi*, Kazuki Koketsu and Hiroe Miyake

Earth, Planets and Space 2019, **71**, 63 DOI: 10.1186/s40623-019-1041-7
Received: 28 February 2019, Accepted: 22 May 2019, Published: 31 May 2019

Abstract

The source rupture process of the 2018 Hokkaido Eastern Iburi earthquake was investigated by performing a joint inversion analysis using the strong motion and geodetic data. A fault model that consists of two fault planes was constructed by considering the relocated aftershock distribution and the focal mechanisms. The inversion result showed that the large slip occurred at approximately 22 km depth, which was much shallower than the hypocentral depth. Our results showed that the rupture initiated on the minor fault plane around the hypocenter and the major fault plane started to rupture 4–6 s after the rupture initiation. Although the shape of the minor fault plane has not been clearly determined, the major fault plane appears to be high-angle, east-dipping. An additional inversion with only the major fault plane showed that the strong ground motion near the source was mainly generated from the major fault plane. The total seismic moment estimated by the inversion with the two fault-plane model was 1.1×10^{19} Nm, which yielded an M_w of 6.6. Using the inversion result of the two fault-plane model, we simulated the ground surface and borehole waveforms at strong motion station IBUH03 where the large velocity pulse was observed on the ground surface. The simulations suggest that this large velocity pulse was generated from the combination of the large slip of the source and large site amplification of the velocity structure between the ground surface and borehole seismometers.

Keywords: Rupture process, 2018 Hokkaido Eastern Iburi earthquake, Strong motion, Geodetic data

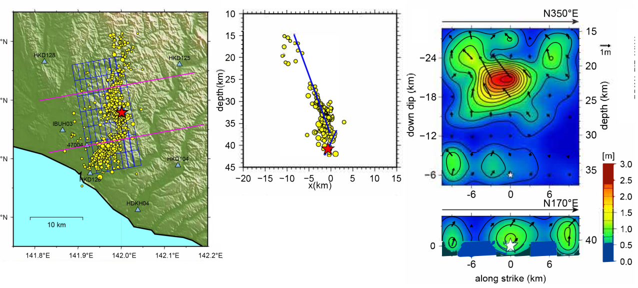

Graphical abstract

*Corresponding author: Hiroaki Kobayashi, kohiroak@kobori-takken.co.jp; khiro@eri.u-tokyo.ac.jp

FULL PAPER **Open Access**

Detection and interpretation of local surface deformation from the 2018 Hokkaido Eastern Iburi Earthquake using ALOS-2 SAR data

Satoshi Fujiwara*, Takayuki Nakano, Yu Morishita, Tomokazu Kobayashi, Hiroshi Yarai, Hiroshi Une and Kyonosuke Hayashi

Earth, Planets and Space 2019, **71**, 64 DOI: 10.1186/s40623-019-1046-2
Received: 5 March 2019, Accepted: 26 May 2019, Published: 3 June 2019

Abstract

We identified and analyzed surface displacements associated with the 2018 Hokkaido Eastern Iburi Earthquake in northern Japan using satellite radar interferograms from the Advanced Land Observing Satellite 2. The data generally show elastic deformation caused by the main earthquake as well as numerous complex surface displacements that cannot be explained by the motion of the seismic source fault. We identified three distinct phenomena: linear surface displacements representing secondary earthquake faults west of the epicenter, surface deformation caused by liquefaction in urban and coastal areas, and coherence changes in the interferograms due to landslides in mountainous areas and liquefaction in urban areas. The linear surface displacements show reverse fault motion with low dip angles and appear to be a geographic extension of known active faults; however, it is unlikely that these displacements were directly connected to the source fault of the main earthquake. Although there is no evidence that they generated strong seismic waves at the time of the main earthquake, there is a possibility that they represent active fault traces and could be the sources of large earthquakes in the future. Therefore, such linear surface displacements can be used to identify potentially dangerous hidden active faults. The interferograms reveal that liquefaction in urban areas occurred in low areas artificially filled during past residential development. Coherence-change maps drawn from the interferograms were useful for detecting liquefaction, but their high sensitivity limited their application for landslide detection in mountainous areas; the phase noise deviation method was more practical for purposes such as rapid response or mitigation. Our methods have the potential to allow improved mapping of local hazards in other areas and can be applied to urban planning and/or safety assessments.

Keywords: 2018 Hokkaido Eastern Iburi Earthquake, ALOS-2, SAR interferometry, Surface fault, Landslide, Liquefaction

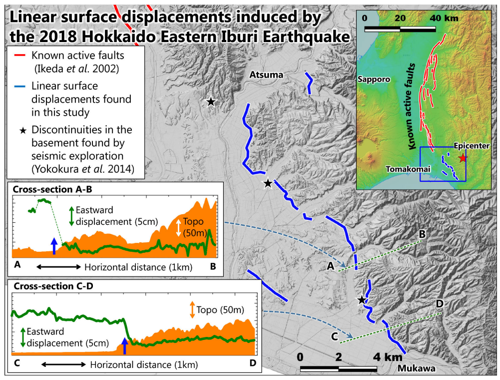

Graphical abstract

*Corresponding author: Satoshi Fujiwara, fujiwara-s2vq@mlit.go.jp

FULL PAPER **Open Access**

Cause of destructive strong ground motion within 1–2 s in Mukawa town during the 2018 M_w 6.6 Hokkaido eastern Iburi earthquake

Nobuo Takai*, Michiko Shigefuji, Jun Horita, Shingo Nomoto, Takahiro Maeda, Masayoshi Ichiyanagi, Hiroaki Takahashi, Hiroaki Yamanaka, Kosuke Chimoto, Seiji Tsuno, Masahiro Korenaga and Nobuyuki Yamada

Earth, Planets and Space 2019, **71**, 67 DOI: 10.1186/s40623-019-1044-4
Received: 5 March 2019, Accepted: 24 May 2019, Published: 13 June 2019

Abstract

We investigated the cause of destructive ground motion during the 2018 Hokkaido eastern Iburi earthquake. We conducted strong motion observations of aftershocks and microtremors and the surface wave method in the damaged areas of the town of Mukawa, Hokkaido prefecture, Japan. The ground accelerations were continuously recorded during a period of approximately 3 months after the main shock on September 6, 2018. The heavily damaged buildings were mainly situated around the strong motion station (HKD126) in Mukawa town. Such concentration of damage can be explained by the strong power that was observed in the 1–2 s period of the response spectrum at this station. We estimated the S-wave velocity profiles of this station site and a temporary station site that was installed on a nearby hill. The estimated S-wave velocity, which was inverted from phase velocity structures with the microtremor array and the surface wave method observations explained the difference in the SH-wave amplification characteristics between the two sites. An analysis of HKD126 and the temporarily observed records clearly indicates the strong effects of the local geological conditions on the heavily damaged area of Mukawa. The strong ground motion power generated during the main shock in Mukawa for 1–2 s period was mainly amplified by this shallow underground velocity structure.

Keywords: The 2018 Hokkaido eastern Iburi earthquake, Strong ground motion, Velocity structure, Temporary strong motion observation, Microtremor measurement, Multichannel analysis of surface wave, S-wave velocity, Site amplification

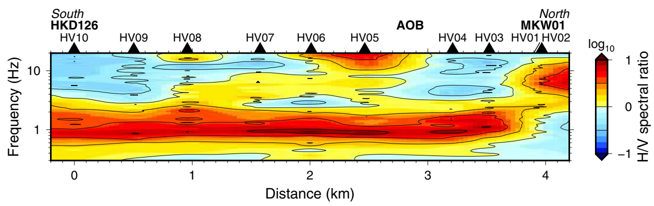

Graphical abstract

*Corresponding author: Nobuo Takai, tki@eng.hokudai.ac.jp

FULL PAPER **Open Access**

Coseismic changes in subsurface structure associated with the 2018 Hokkaido Eastern Iburi Earthquake detected using autocorrelation analysis of ambient seismic noise

Hiroki Ikeda and Ryota Takagi*

Earth, Planets and Space 2019, **71**, 72 DOI: 10.1186/s40623-019-1051-5
Received: 24 February 2019, Accepted: 18 June 2019, Published: 27 June 2019

Abstract

Autocorrelation analysis using ambient noise is a useful method to detect temporal changes in wave velocity and scattering property. In this study, we investigated the temporal changes in seismic wave velocity and scattering property in the focal region of the 2018 Hokkaido Eastern Iburi Earthquake. The autocorrelation function (ACF) was calculated by processing with bandpass filters to enhance 1–2 Hz frequency range, with aftershock removal, and applying the one-bit correlation technique. The stretching method was used to detect the seismic wave velocity change. After the mainshock, seismic velocity reductions were observed at many stations. At N. AMAH and ATSUMA, which are located close to the mainshock, we detected 2–3% decreases in seismic wave velocity. We compared parameters indicating strong ground motion and showed the possibility of correlations with peak dynamic strain and seismic velocity reduction. We also investigated the relationship between waveform correlation and lag time, using ACFs from before and after the mainshock, and detected distortion of the ACF waveform. The source of the waveform decorrelation was estimated to be located near the maximum coseismic slip, at around 30 km depth. Thus, distortion of the ACF waveform may reflect the formation of cracks, due to faulting at approximately 30 km depth.

Keywords: Seismic velocity changes, Ambient noise, Scatterer distribution change, Autocorrelation function, Hokkaido Eastern Iburi Earthquake, Seismic interferometry

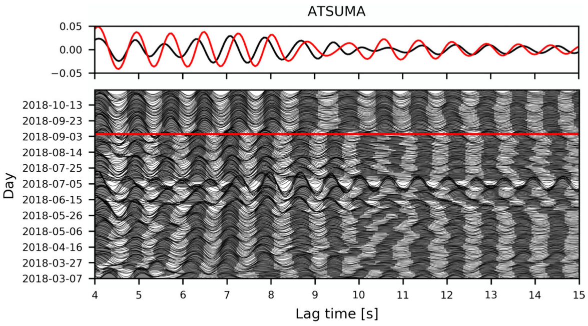

Graphical abstract

*Corresponding author: Ryota Takagi, ryota.takagi.c1@tohoku.ac.jp

FULL PAPER **Open Access**

Topographic effects on frequency-size distribution of landslides triggered by the Hokkaido Eastern Iburi Earthquake in 2018

Mio Kasai* and Takashi Yamada

Earth, Planets and Space 2019, **71**, 89 DOI: 10.1186/s40623-019-1069-8
Received: 18 February 2019, Accepted: 6 August 2019, Published: 17 August 2019

Abstract

This study examined the frequency-size distribution of 6117 landslides spread over 440 km^2 in Iburi Subprefecture, Hokkaido, Japan, induced by the Hokkaido Eastern Iburi Earthquake (M_w 6.6) on September 6, 2018. The study area is characterized by gently undulating terrain that is finely dissected by shallow streams and covered predominantly by layers of volcanic products with high water content. Most of the landslides were shallow landslides, and their slip surfaces often formed in a layer of volcanic soil called the "Ta-d," deposited at 9000 ybp. Low ridges separating small catchments allowed individual landslides to coalesce in many locations. The average size of landslides was 7160 m^2. Landslide size tended to increase with slope angle up to 20° to 25° and then decrease with further increase of slope angle. About half of the landslides occurred in a feature with both concave planform and profile curvature, and their average size was 8720 m^2. In contrast, 17% of the total landslides occurred in the case of both curvatures being convex, and their average size was 5190 m^2. The results indicated that the accumulation of saturated soil in concave features provided more opportunities for landslides of large sizes. The frequency-size distribution of the landslides presented high rollover, 5.0×10^{-3} km^2, but the exponent of power law decay for medium to large landslides, −2.46, was not largely different from those of studies in other locations. Compared with other seismically caused examples, the landslides triggered by the Hokkaido Eastern Iburi Earthquake can be characterized as more clustered, more numerous, and larger in size for the moment magnitude of the earthquake. Conversely, the magnitude scale for the landslide event estimated from the total landslide area was equivalent to that of a region struck by an earthquake of $M_w = 7.0$ to 7.4. This study demonstrated that gently undulating regions can produce unexpectedly large and frequent landslides when struck by an intense earthquake, and when soil layers vulnerable to ground shaking cover the ground.

Keywords: Frequency-size distribution, Hokkaido Eastern Iburi Earthquake, Shallow landslides, Slope angle, Slope curvature, Volcanic soil

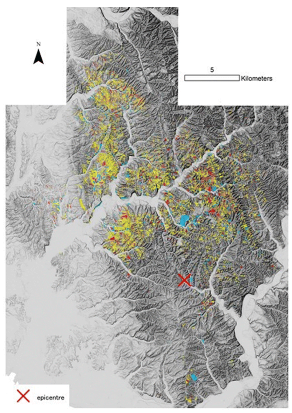

Graphical abstract

*Corresponding author: Mio Kasai, kasaim@for.agr.hokudai.ac.jp

FULL PAPER Open Access

Source rupture process of the 2018 Hokkaido Eastern Iburi earthquake deduced from strong-motion data considering seismic wave propagation in three-dimensional velocity structure

Kimiyuki Asano* and Tomotaka Iwata

Earth, Planets and Space 2019, **71**, 101 DOI: 10.1186/s40623-019-1080-0
Received: 1 May 2019, Accepted: 3 September 2019, Published: 18 September 2019

Abstract

The source rupture process of the 2018 Hokkaido Eastern Iburi earthquake (M_{JMA} 6.7) was analyzed by a kinematic waveform inversion method using strong-motion data in 0.04–0.5 Hz. This earthquake occurred close to the Hidaka Collision Zone and the Ishikari depression, where the crustal structure is rather complex. Thus, we used a three-dimensional velocity structure model to compute the theoretical Green's functions by the finite difference method. A source fault model with strike-angle variation was set based on the spatial distribution of the early aftershocks. The strong-motion stations used for the source inversion were selected based on the result of forward ground motion simulation of a moderate aftershock. The slip in the first 5 s was relatively small, but an area of significant slip with peak slip of 1.7 m was found in the depth range from 22 to 32 km. The rupture propagated upward mainly in the southwest direction. Based on the regional crustal structure and the configuration of the Moho discontinuity, the large-slip area was thought to be located in the lower crust, and its rupture did not reach the upper part of the continental crust. Most of the early aftershocks occurred around the large-slip area. The later aftershocks at the depth shallower than 20 km occurred outside the causative source fault of the mainshock. Three-dimensional ground motion simulation demonstrated that the heterogeneous source process and the three-dimensional basin and crustal velocity structure brought a large velocity pulse to an area to the southwest of the source fault, where the largest PGV was observed during the mainshock. The spatial distribution of the simulated PGV resembled the observed PGV distribution except some sites located inside the Ishikari depression where thick Quaternary soft low-velocity sediments exist at the top of the basin.

Keywords: The 2018 Hokkaido Eastern Iburi earthquake, Source rupture process, Kinematic source inversion, Strong-motion data, Three-dimensional velocity structure, Ground motion simulation

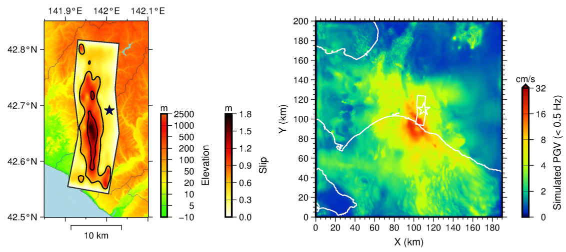

Graphical abstract

*Corresponding author: Kimiyuki Asano, k-asano@sms.dpri.kyoto-u.ac.jp

FULL PAPER Open Access

Characteristics of relocated hypocenters of the 2018 M6.7 Hokkaido Eastern Iburi earthquake and its aftershocks with a three-dimensional seismic velocity structure

Saeko Kita

Earth, Planets and Space 2019, **71**, 122 DOI: 10.1186/s40623-019-1100-0
Received: 1 May 2019, Accepted: 27 October 2019, Published: 14 November 2019

Abstract

I relocated the hypocenters of the 2018 M6.7 Hokkaido Eastern Iburi earthquake and its surrounding area, using a three-dimensional seismic structure, the double-difference relocation method, and the JMA earthquake catalog. After relocation, the focal depth of the mainshock became 35.4 km. As previous studies show, in south-central Hokkaido, the Hidaka collision zone is formed, and anomalous deep and thickened forearc crust material is subducting at depths of less than 70 km. The mainshock and its aftershocks are located at depths of approximately 10 to 40 km within the lower crust of the anomalous deep and thickened curst near the uppermost mantle material intrusions in the northwestern edge of this Hidaka collision zone. Like the two previous large events, the aftershocks of this event incline steeply eastward and appear to be distributed in the deeper extension of the Ishikari-teichi-toen fault zone. The highly inclined fault in the present study is consistent with a fault model by a geodetic analysis with InSAR. The aftershocks at depths of 10 to 20 km are located at the western edge of the high-attenuation (low-Qp) zone. These kinds of relationships between hypocenters and materials are the same as the 1970 and 1982 events in the Hidaka collision zone. The anomalous large focal depths of these large events compared with the average depth limit of inland earthquakes in Japan could be caused by the locally lower temperature in south-central Hokkaido. This event is one of the approximately M7 large inland earthquakes that occurred repeatedly at a recurrence interval of approximately 40 years and is important in the collision process in the Hidaka collision zone.

Keywords: Relocations of hypocenters, The Hidaka collision zone, Hokkaido, Seismic structures

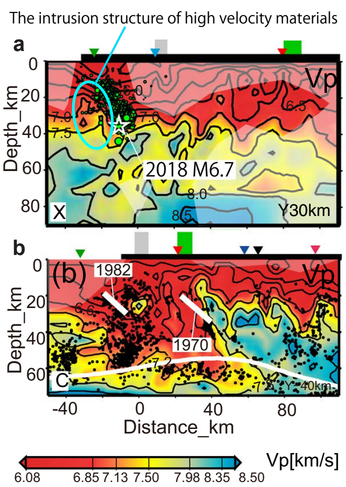

Graphical abstract

Corresponding author: Saeko Kita, kita@kenken.go.jp

FULL PAPER **Open Access**

Characteristics of seismic activity before and after the 2018 M6.7 Hokkaido Eastern Iburi earthquake

Takao Kumazawa*, Yosihiko Ogata and Hiroshi Tsuruoka

Earth, Planets and Space 2019, **71**, 130 DOI: 10.1186/s40623-019-1102-y
Received: 25 April 2019, Accepted: 29 October 2019, Published: 29 November 2019

Abstract

We applied the epidemic type aftershock sequence (ETAS) model, the two-stage ETAS model and the non-stationary ETAS model to investigate the detailed features of the series of earthquake occurrences before and after the M6.7 Hokkaido Eastern Iburi earthquake on 6 September 2018, based on earthquake data from October 1997. First, after the 2003 M8.0 Tokachi-Oki earthquake, seismic activity in the Eastern Iburi region reduced relative to the ETAS model. During this period, the depth ranges of the seismicity were migrating towards shallow depths, where a swarm cluster, including a M5.1 earthquake, finally occurred in the deepest part of the range. This swarm activity was well described by the non-stationary ETAS model until the M6.7 main shock. The aftershocks of the M6.7 earthquake obeyed the ETAS model until the M5.8 largest aftershock, except for a period of several days when small, swarm-like activity was found at the southern end of the aftershock region. However, when we focus on the medium and larger aftershocks, we observed quiescence relative to the ETAS model from 8.6 days after the main shock until the M5.8 largest aftershock. For micro-earthquakes, we further studied the separated aftershock sequences in the naturally divided aftershock volumes. We found that the temporal changes in the background rate and triggering coefficient (aftershock productivity) in respective sub-volumes were in contrast with each other. In particular, relative quiescence was seen in the northern deep zones that includes the M5.8 largest aftershock. Furthermore, changes in the *b*-values of the whole aftershock activity showed an increasing trend with respect to the logarithm of elapsed time during the entire aftershock period, which is ultimately explained by the spatially different characteristics of the aftershocks.

Keywords: ABIC, AIC, Bayesian method, *b*-Values, Stationary ETAS model, Two-stage ETAS model, Non-stationary ETAS model

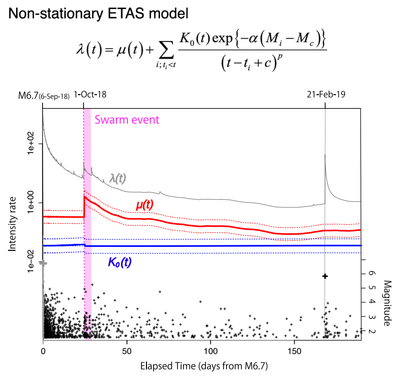

Graphical abstract

*Corresponding author: Takao Kumazawa, tkuma@eri.u-tokyo.ac.jp

EXPRESS LETTER **Open Access**

Spatiotemporal crustal strain distribution around the Ishikari-Teichi-Toen fault zone estimated from global navigation satellite system data

Mako Ohzono*, Hiroaki Takahashi and Chihiro Ito

Earth, Planets and Space 2019, **71**, 50 DOI: 10.1186/s40623-019-1024-8
Received: 3 February 2019, Accepted: 6 April 2019, Published: 27 April 2019

Abstract

Based on analyses of global navigation satellite system data since 1996, we investigate the spatiotemporal strain field around the Ishikari-Teichi-Toen fault zone, which is a major active fault zone close to the epicenter of the 2018 Eastern Iburi earthquake in Hokkaido, Japan. Strain rates during almost whole periods, except for the timings of two distant large interplate earthquakes and following several years show an E–W to ESE–WNW contraction of ~ 0.1 ppm/year. This strain rate is approximately an order of magnitude larger than that of the surrounding area. Strain rate disturbances due to large earthquakes diminish within several years and return to the original level, suggesting that there is a uniform strain accumulation along this fault zone. Strain rate profiles that traverse the fault zone are characterized by a major contraction, corresponding to the Ishikari lowlands where a significantly thick low seismic velocity layer exists. A relatively high strain rate around this fault zone may reflect some amount of inelastic strain accumulation in addition to the elastic strain accumulation along the faults originating from complex fault and crustal structures.

Keywords: 2018 Eastern Iburi earthquake, Ishikari lowlands, GNSS, Strain concentration zone, Active faults

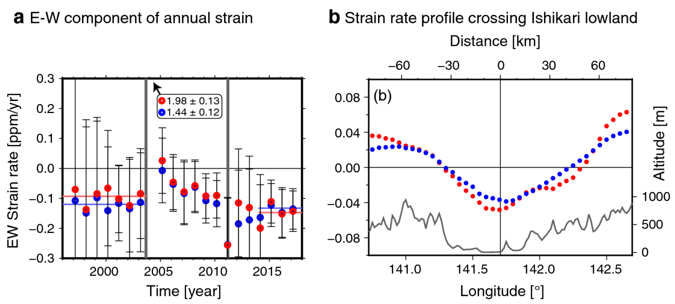

Graphical abstract

*Corresponding author: Mako Ohzono, m.ohzono@sci.hokudai.ac.jp

EXPRESS LETTER **Open Access**

The 2018 Hokkaido Eastern Iburi earthquake ($M_{JMA}=6.7$) was triggered by a strike-slip faulting in a stepover segment: insights from the aftershock distribution and the focal mechanism solution of the main shock

Kei Katsumata*, Masayoshi Ichiyanagi, Mako Ohzono, Hiroshi Aoyama, Ryo Tanaka, Masamitsu Takada, Teruhiro Yamaguchi, Kazumi Okada, Hiroaki Takahashi, Shin'ichi Sakai, Satoshi Matsumoto, Tomomi Okada, Toru Matsuzawa, Shuichiro Hirano, Toshiko Terakawa, Shinichiro Horikawa, Masahiro Kosuga, Hiroshi Katao, Yoshihisa Iio, Airi Nagaoka, Noriko Tsumura, Tomotake Ueno and the Group for the Aftershock Observations of the 2018 Hokkaido Eastern Iburi Earthquake

Earth, Planets and Space 2019, **71**, 53 DOI: 10.1186/s40623-019-1032-8
Received: 24 December 2018, Accepted: 23 April 2019, Published: 20 May 2019

Abstract

The Hokkaido Eastern Iburi earthquake ($M_{JMA}=6.7$) occurred on September 6, 2018, in the Hokkaido corner region where the Kurile and northeastern Japan island arcs meet. We relocated aftershocks of this intraplate earthquake immediately after the main shock by using data from a permanent local seismic network and found that aftershock depths were concentrated from 20 to 40 km, which is extraordinarily deep compared with other shallow intraplate earthquakes in the inland area of Honshu and Kyushu, Japan. Further, we found that the aftershock area consists of three segments. The first segment is located in the northern part of the aftershock area, the second segment lies in the southern part, and the third segment forms a stepover between the other two segments. The hypocenter of the main shock, from which the rupture initiated, is located on the stepover segment. The centroid moment tensor solution for the main shock indicates a reverse faulting, whereas the focal mechanism solution determined by using the first-motion polarity of the *P* wave indicates strike-slip faulting. To explain this discrepancy qualitatively, we present a model in which the rupture started as a small strike-slip fault in the stepover segment of the aftershock area, followed by two large reverse faulting ruptures in the northern and southern segments.

Keywords: The Hokkaido Eastern Iburi earthquake, Strike-slip fault, Reverse fault, Aftershock distribution, Focal mechanism solution, Local seismic network, Stepover segment

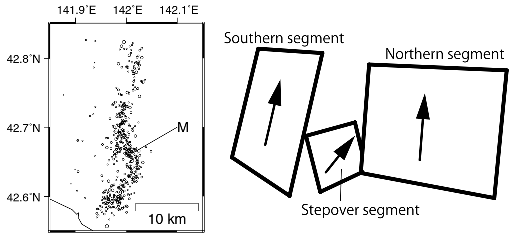

Graphical abstract

*Corresponding author: Kei Katsumata, kkatsu@sci.hokudai.ac.jp

EXPRESS LETTER **Open Access**

Geodetically estimated location and geometry of the fault plane involved in the 2018 Hokkaido Eastern Iburi earthquake

Tomokazu Kobayashi*, Kyonosuke Hayashi and Hiroshi Yarai

Earth, Planets and Space 2019, **71**, 62 DOI: 10.1186/s40623-019-1042-6
Received: 6 March 2019, Accepted: 22 May 2019, Published: 31 May 2019

Abstract

By applying the InSAR method to ALOS-2 SAR data acquired before and after the 2018 Hokkaido Eastern Iburi earthquake, the ground displacement fields were successfully mapped. Ground deformation is distributed on the eastern side of an active fault, known as the Ishikari-Teichi-Toen fault zone (ITTFZ). Uplift of up to ~ 7 cm is distributed throughout the source region, and eastward movement of up to ~ 4 cm is widely observed on the eastern side of the source region. The fault model constructed by inverting InSAR and GNSS data under an assumption of a uniform slip on a rectangular fault plane shows reverse fault motion on a plane dipping eastward at 74°. The fault top is positioned around a depth of 15 km, suggesting that the slip significantly occurs deeper than the typical seismogenic zone for the Japanese island. The fault plane is at a relatively high dip angle, and the shallow extension of the estimated fault plane does not connect to any known surface traces of the ITTFZ. This may suggest that the fault involved with the 2018 event is physically separated from the ITTFZ, or that the fault plane bends to a lower dip angle at a shallow crustal depth. The fault rupture area is located in a spatially inhomogeneous seismic velocity structure field and the main slip occurs at the western edge of a low Vp area which vertically thickens on the eastern side of the fault. This may suggest that the 2018 earthquake occurred at seismic velocity boundary. An estimate of Coulomb Failure Function change suggests that the static stress change due to the 2018 event can promote reverse fault slip on the southern part of the ITTFZ.

Keywords: 2018 Hokkaido Eastern Iburi earthquake, Crustal deformation, InSAR, Fault model

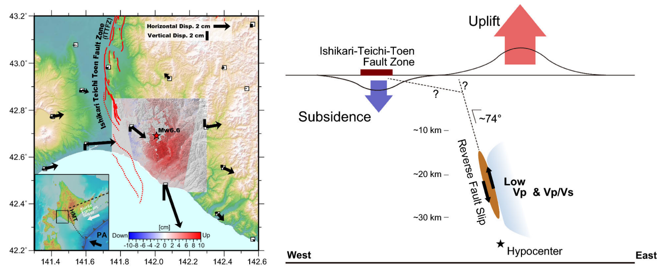

Graphical abstract

*Corresponding author: Tomokazu Kobayashi, kobayashi-t96dv@mlit.go.jp

EXPRESS LETTER Open Access

Source parameters and site amplifications estimated by generalized inversion technique: focusing on the 2018 Hokkaido Iburi-Tobu earthquake

Kenichi Nakano* and Hiroshi Kawase

Earth, Planets and Space 2019, **71**, 66 DOI: 10.1186/s40623-019-1047-1
Received: 24 February 2019, Accepted: 4 June 2019, Published: 13 June 2019

Abstract

The 2018 Hokkaido Iburi-Tobu earthquake occurred on September 6. In this earthquake, seismic intensity 7 was measured at Shikanuma, Atsuma Town, and severe damage occurred in Hokkaido. The strong motions were recorded at observation stations including those nearby the epicenter, and the seismograms at a few stations close to the epicenter showed pulse-like waveforms. In the region called Yufutsu Plain, the underground structure is quite complex because Yufutsu Plain is located at the western margin of the Hidaka collision zone. Thus, the mechanism of generating the observed high-amplitude ground motions in this area has not been clarified yet. We performed the generalized inversion technique to estimate the fundamental characteristics of source terms and site amplifications at Yufutsu area to investigate the mechanism mentioned above. We found that the stress drop of the mainshock of the 2018 Hokkaido Iburi-Tobu earthquake was approximately 10Mpa, which corresponds to the upper limit of the crustal earthquakes in the past, and that the short-period level *A* was approximately 1.17×10^{19} N·m. We also evaluated the site amplification at sites close to the aftershock zone. We found that the sites in the north with relatively high altitudes showed dominant frequencies above several Hz, while the sites in the south with relatively low altitudes showed dominant frequencies of approximately 1 Hz or lower. We also found that the site amplifications were quite large at three sites (BBC, HKD126 and IBUH03) where we observed clear pulse-like waveforms, and confirmed that they all showed dominant frequencies at approximately 1 Hz.

Keywords: 2018 Hokkaido Iburi-Tobu earthquake, Stress drop, Short-period level *A*, Site amplification

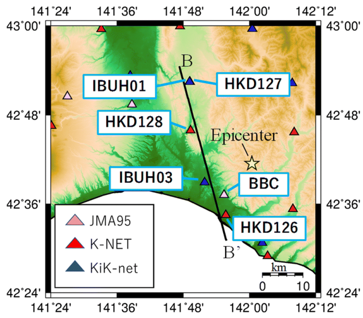

Graphical abstract

*Corresponding author: Kenichi Nakano, nakano.kenichi@ad-hzm.co.jp

EXPRESS LETTER Open Access

Estimation of convergence boundary location and velocity between tectonic plates in northern Hokkaido inferred by GNSS velocity data

Chihiro Ito*, Hiroaki Takahashi and Mako Ohzono

Earth, Planets and Space 2019, **71**, 86 DOI: 10.1186/s40623-019-1065-z
Received: 26 February 2019, Accepted: 24 July 2019, Published: 2 August 2019

Abstract

The present location of the tectonic boundary and the convergence rate between the Amur and Okhotsk plates in northern Hokkaido, Japan, were herein estimated from the velocity field using data from a continuous GNSS network. The observed velocity profiles are in agreement with the theoretical ones calculated from a tectonic block collision model. The estimated kinematic boundary agrees with both geological and seismic boundaries. Overall, this indicates that the geological boundary acts like a mechanical one. The calculated convergence velocity of 14.0–16.5 mm/year is consistent with predictions from regional plate motion models and suggests that a considerable amount of interplate convergence is in progress along this boundary. Deep crustal seismicity is also in agreement with the estimated elastic thickness of 20.5–25.5 km. The non-occurrence of large earthquakes during the past several centuries, and the estimated convergence velocity suggest that there is a high potential for a large event in the near future.

Keywords: GNSS measurements, Collision zone, Amur plate, Crustal deformation, Hokkaido

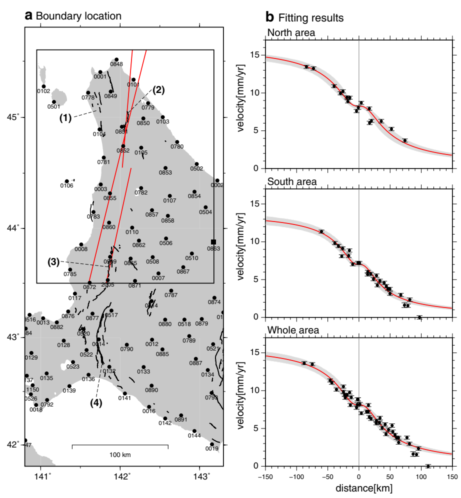

Graphical abstract

*Corresponding author: Chihiro Ito, chr-0521-i@eis.hokudai.ac.jp

EXPRESS LETTER **Open Access**

Electrical resistivity modeling around the Hidaka collision zone, northern Japan: regional structural background of the 2018 Hokkaido Eastern Iburi earthquake (M_w 6.6)

Hiroshi Ichihara*, Toru Mogi, Hideyuki Satoh and Yusuke Yamaya

Earth, Planets and Space 2019, **71**, 100 DOI: 10.1186/s40623-019-1078-7
Received: 5 March 2019, Accepted: 26 August 2019, Published: 18 September 2019

Abstract

The Hidaka collision zone, the collision boundary between the NE Japan and Kurile arcs, is known to be an ideal region to study the evolution of island arcs. The hypocenter of the 2018 Hokkaido Eastern Iburi earthquake (M_w 6.6) in the western part of the Hidaka collision zone was unusually deep for an inland earthquake, and the reverse fault that caused the earthquake has an uncharacteristically steep dip. In this study, we used three-dimensional inversion to reanalyze broadband magnetotelluric data acquired in the collision zone. The inverted resistivity model showed a significant area of high resistivity around the center of the collision boundary. We also identified a conductive zone beneath an area of serpentinite mélange in a zone of high *P*–*T* metamorphic rocks west of the high-resistivity zone. The conductive zone possibly reflects areas rich in pore fluids related to the formation and elevation of the serpentinites. Sensitivity tests indicated the need for additional magnetotelluric survey data to delineate the resistivity distribution around the epicentral area of the 2018 earthquake although the resistivity model showed a conductive zone in this area.

Keywords: Hidaka collision zone, Magnetotellurics, Electrical conductivity, Resistivity, Serpentinite, 2018 Hokkaido Eastern Iburi earthquake

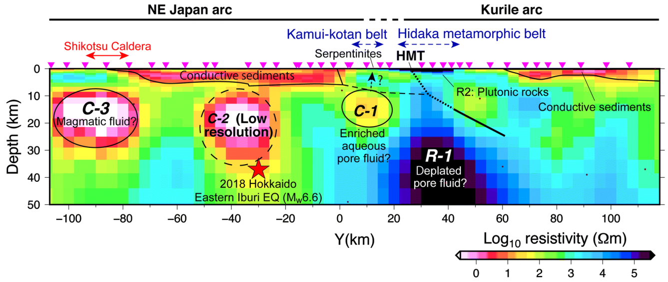

Graphical abstract

*Corresponding author: Hiroshi Ichihara, h-ichi@seis.nagoya-u.ac.jp

EXPRESS LETTER **Open Access**

Three-dimensional S-wave attenuation structure in and around source area of the 2018 Hokkaido Eastern Iburi Earthquake, Japan

Ryoichi Nakamura* and Takahiro Shiina

Earth, Planets and Space 2019, **71**, 114 DOI: 10.1186/s40623-019-1095-6
Received: 8 May 2019, Accepted: 23 October 2019, Published: 6 November 2019

Abstract

We investigate S-wave attenuation (Qs) structure in and around Hokkaido, Japan, including the source area of the 2018 Hokkaido Eastern Iburi Earthquake (M 6.7) and its aftershocks. From the strong-motion seismograms recorded in the nationwide seismograph network in Japan, we compute spectrum amplitude at 1–10 Hz with every 1 Hz and then estimate Qs structure by adopting tomographic inversion technique. The obtained Qs structure suggests that lateral variations of Qs are remarkably formed in the study areas. The low-Qs anomalies distributing north to south are imaged in both sides of the Hidaka mountain range which is built in the central Hokkaido. These characteristics structures of Qs are extended from the ground surface to depths by about 50 km, indicating that heterogeneous structures resulted from the collision of the Kuril and northeastern Japan arcs develop at the depth ranges. Around the source area of the 2018 Hokkaido Eastern Iburi Earthquake, the abrupt changes of Qs values are identified. The 2018 Hokkaido Eastern Iburi Earthquake and its aftershocks seem to be arraigned on the high-Qs zones, whereas the low-Qs anomalies are also imaged next to the high-Qs zones. The boundary of the low- and high-Qs zones lies with near vertical, corresponding to aftershock distributions of the 2018 Hokkaido Eastern Iburi Earthquake. This agreement would propose that the heterogeneities formed due to the arc–arc collision would characterize faulting processes in the main shock of the Hokkaido Eastern Iburi Earthquake and the activities of its aftershocks.

Keywords: The 2018 Hokkaido Eastern Iburi Earthquake, S-wave attenuation, The arc–arc collision zone, Tomography

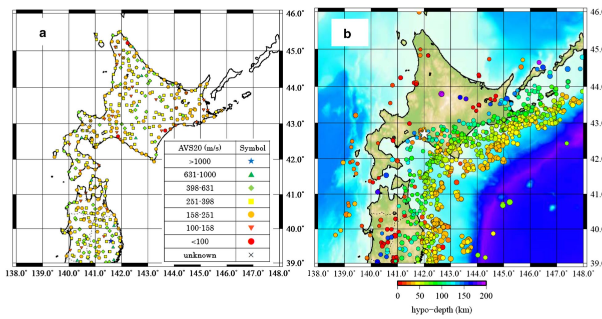

Fig. 1

*Corresponding author: Ryoichi Nakamura, naka@eri.u-tokyo.ac.jp

EXPRESS LETTER **Open Access**

Estimation of the source process and forward simulation of long-period ground motion of the 2018 Hokkaido Eastern Iburi, Japan, earthquake

Hisahiko Kubo*, Asako Iwaki, Wataru Suzuki, Shin Aoi and Haruko Sekiguchi

Earth, Planets and Space 2020, **72**, 20 DOI: 10.1186/s40623-020-1146-z
Received: 24 December 2019, Accepted: 30 January 2020, Published: 18 February 2020

Abstract

In this study, we investigate the source rupture process of the 2018 Hokkaido Eastern Iburi earthquake in Japan (M_{JMA} 6.7) and how the ground motion can be reproduced using available source and velocity models. First, we conduct a multiple-time-window kinematic waveform inversion using strong motion waveforms, which indicates that a large slip area located at a depth of 25–30 km in the up-dip direction from the hypocenter was caused by a rupture propagating upward 6–12 s after its initiation. Moreover, the high-seismicity area of aftershocks did not overlap with the large-slip area. Subsequently, using the obtained source model and a three-dimensional velocity structure model, we conduct a forward long-period (< 0.5 Hz) ground-motion simulation. The simulation was able to reproduce the overall ground-motion characteristics in the sedimentary layers of the Ishikari Lowland.

Keywords: The 2018 Hokkaido Eastern Iburi earthquake, Source process, Forward simulation, Long-period ground motion

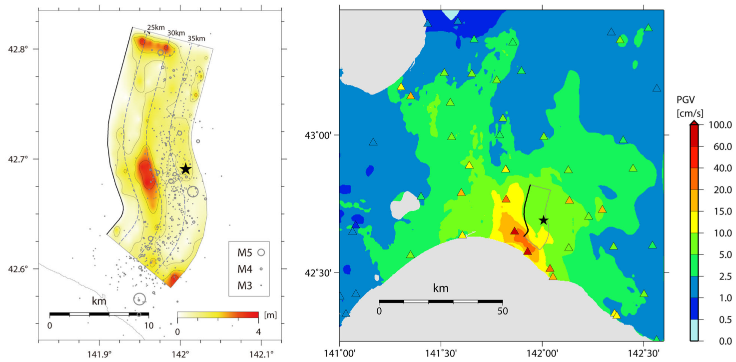

Graphical abstract

*Corresponding author: Hisahiko Kubo, hkubo@bosai.go.jp

EXPRESS LETTER **Open Access**

Coseismic changes in groundwater level during the 2018 Hokkaido Eastern Iburi earthquake

Tomo Shibata*, Ryo Takahashi, Hiroaki Takahashi, Takanori Kagoshima, Naoto Takahata, Yuji Sano and Daniele L. Pinti

Earth, Planets and Space 2020, **72**, 23 DOI: 10.1186/s40623-020-01152-y
Received: 24 May 2019, Accepted: 17 February 2020, Published: 26 February 2020

Abstract

Six wells were continuously monitored in Hokkaido, northern Japan, to relate groundwater level changes to regional seismic activity. Groundwater level changes following the 2018 Hokkaido Eastern Iburi earthquake were detected in three of the six wells, even though they are located hundreds of kilometers from the epicenter. The groundwater level changes are qualitatively consistent with the volumetric strain induced by the earthquake. We analyzed groundwater level responses to the M_2 tidal constituent before and after the earthquake, but related changes in amplitude and phase shifts remained within the usual variation. Observed coseismic change was explained by the response to the M_2 tidal constituent component and the calculated volumetric strain for one of the wells, where groundwater level decreased. The observed change in the other two was found to be much greater than the corresponding estimates of the volumetric strain.

Keywords: Groundwater level, Coseismic change, 2018 Hokkaido Eastern Iburi earthquake, Tidal response

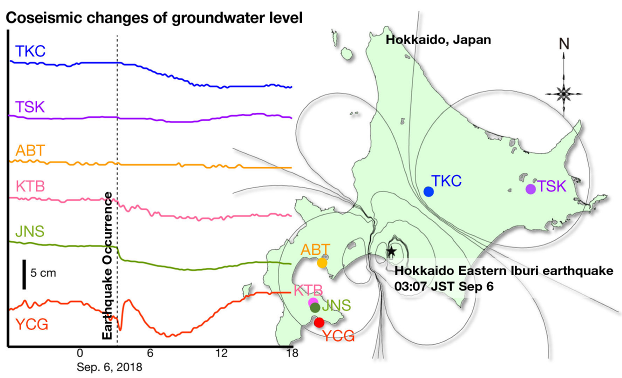

Graphical abstract

*Corresponding author: Tomo Shibata, swn05-toshibat@bep.vgs.kyoto-u.ac.jp

Information for Contributors

General

1. Manuscripts should be submitted through the journal's Editorial Manager system (https://www.editorialmanager.com/epsp/default.aspx).
2. Only papers not previously published will be accepted, and the emphasis is on the originality of concept or observation.
3. Five varieties of article types are available.
   - 3.1 "Full Paper" without word limit.
   - 3.2 "Express Letter" has a limit of 5000 words including the main text, figure legends and table legends. The sum of the number of figures and tables should be less than or equal to 5.
   - 3.3 "Frontier Letter" can be submitted upon invitation by the Editor-in-Chief.
   - 3.4 "Technical Report" describes the technical development of instrument or software.
   - 3.5 "Comment" is a substantial re-analysis of a previously published article in the journal. "Comment" should not exceed 1000 words.
4. Authors retain the copyright, and distribution of articles is free under the CC BY license.

Technical

1. Manuscripts should be written in English with double spacing.
2. Each manuscript should be organized in the following order: title, authors' names, affiliations, abstract, key words, main text, acknowledgement, appendix, references, and supplementary materials. A graphical abstract image must be uploaded during submission which should provide the reader with a visual description of the topic covered in the article.
3. The corresponding author should be clearly indicated.
4. The abstract is limited to 350 words and should be informative and include principal findings and conclusions. Please avoid abbreviations.
5. The main text can have multiple free headings.
6. High-resolution figures should be provided in the following format; PDF (preferred format for diagrams), PNG (preferred format for photos or images), EPS ,TIFF, JPEG, BMP. The graphical abstract should be approximately 920×300 pixels and should be uploaded as a JPEG, PNG or SVG file.
7. References must follow the Springer Basic style.

Correspondence

If you have any questions, please contact info@springeropen.com.

A Grant-in-Aid for Publication of Scientific Research Results (19HP1001) from Japan Society for the Promotion of Science is used for printing.

Contents

Cover image: Iwasaki, T. *et al.*, *Earth, Planets and Space* 2019, **71**:103 DOI: 10.1186/s40623-019-1081-z